Korean J. of Chem. Eng., **12**(1), 72-79 (1995)

INTRAPARTICLE TRANSPORT OF AMINO ACIDS IN A CATION EXCHANGER

Cheol Min Kim, Jeong Hee Kang and Hee Moon†

Department of Chemical Technology, Chonnam National University, Kwangju 500-757, Korea
(Received 15 March 1994 • accepted 20 July 1994)

Abstract—Intraparticle transport of amino acids, phenylalanine and tyrosine, in a macroreticular cation-exchange resin, Amberlite 200, was investigated in a finite batch adsorber. A transport model was developed based on the consecutive diffusion of the amino acids through liquid-filled macropores and microspheres. The latter was further simplified by the linear driving force approximation (LDFA) since the microspheres are quite small. The model was used satisfactorily for simulating and predicting the performance of finite batch operations.

Key words: Intraparticle Transport, Phenylalanine and Tyrosine, Cation Exchanger, Finite Batch Operation

INTRODUCTION

Amino acids are usually amphoteric. They exist both as anions and cations, depending upon the solution pH [1]. Therefore adsorption and desorption of amino acids from ion-exchange resins may be carried out by adjusting the solution pH. A cation resin can easily take up an amino acid at a pH value in which the amino acid is positively charged, but it would be regenerated by changing the solution pH to a new value at which the amino acid is negatively charged. Such a character makes it possible to recover and concentrate an amino acid from dilute mixed solutions by means of a cyclic operation with solutions of different pH values [2, 3].

Ion-exchange has been the most widely used technology in various stages of the separation process for the industrial production of amino acids [1]. Many researchers have addressed the effect of equilibrium on the dynamics of ion-exchange processes for the separation of amino acids. Seno and Yamabe [4] have examined the uptake of amino acids by both cation- and anion exchange resins and Feitelson [5] has investigated the uptake of amino acids at their isoelectric pH. Recently Yu et al. [6, 7] have studied the equilibrium and dynamic behavior of ion-exchange columns to obtain optimum design values for separation processes.

While ion-exchange resins have been used in various industrial processes, few studies have been made on the basic features of mass transfer characteristics in ion-exchange operations. Transport in gel-type resins is well understood but the transport in macroreticular ion-exchange resins is not easily understood since they consist of an agglomerate of microspherical gel particles [8]. At the present state of knowledge, intraparticle transport in macroreticular resins may occur by means of two mechanisms, diffusion through the liquid-filled macropores and transport into the microspheres. Yoshida et al. [9] mentioned that while at low solution concentrations diffusion through microspheres is dominant, at higher concentrations diffusion through liquid-filled macropores is dominant.

In this study, we used a commercial cation exchanger, Amberlite 200, which is a polystyrene-based macroreticular resin cross-linked with divinylbenzene (DVB). Amino acids used are L-phenylalanine and L-tyrosine which have quite a similar isoelectric pH. In this case, the difference in specific affinity may be a major cause for the separation of amino acids. Equilibrium uptake of each amino acid has been obtained experimentally as a function of its concentration and solution pH. An ion-exchange equilibrium model, which takes into account the heterogeneity of functional groups in the ion-exchange resin, was used. A transport model was developed based on the consecutive diffusion of the amino acids through liquid-filled macropore and microspheres and it was incorporated with the ion-exchange equilibrium model to form a separation model for batch operations.

THEORETICAL APPROACH

1. Solution Equilibria

Amino acids, which are represented as $NH_2CHRCOOH$, exist both as anions and cations depending on the solution pH. Therefore equilibrium dissociation reactions take place along a certain range of pH values of aqueous solutions. For special cases in which amino acids have functional groups without an additional dissociation reaction and form an ideal solution, the concentrations of charged amino acids can be calculated from the following equations.

$$C_{Ai}^{+} = \frac{C_{Ai}}{\left(1+\frac{K_1}{C_{H^+}}+\frac{K_1K_2}{(C_{H^+})^2}\right)} \tag{1}$$

$$C_{Ai}^{-} = \frac{C_{Ai}}{\left(1+\frac{C_{H^+}}{K_2}+\frac{(C_{H^+})^2}{K_1K_2}\right)} \tag{2}$$

where C_{Ai} is the total concentration of the i-th amino acid and K_1 and K_2 are the dissociation constants. The solution pH may be calculated from the electroneutrality condition. If amino acids exist in a salt solution such as NaCl, it can be expressed as follows

$$\sum_i C_{Ai}^{+} + C_{Na^+} + C_{H^+} = \sum_i C_{Ai}^{-} + C_{Cl^-} + C_{OH^-} \tag{3}$$

†Author to whom all correspondences should be made.

C_{OH}^- is the concentration of hydroxyl ion, which can be calculated from the dissociation product of water. The solution pH and concentrations of each charged amino acid can be obtained by a trial and error solution of the simultaneous equations above. When the solution pH is known, the concentrations of charged amino acids can be simply calculated from Eqs. (1) and (2). The ionic fraction of C_{Ai}^+ is usually defined by

$$X_{Ai}=\frac{C_{Ai}^+}{\sum_j C_{Aj}^+ + C_{Na}^+ + C_H^+} \tag{4}$$

and the apparent selectivity for the ion-exchange of C_{Ai}^+ and C_{Aj}^+ is defined by the following equation

$$S_{i,j}=\left(\frac{Y_{Ai}}{X_{Ai}}\right)/\left(\frac{Y_{Aj}}{X_{Aj}}\right) \tag{5}$$

The ionic fraction of C_{Ai}^+ taken by the ion exchange is defined by

$$Y_{Ai}=Q_i/Q_0 \tag{6}$$

where Q_i is the amount of C_{Ai}^+ taken by the resin and Q_0 is the ion-exchange capacity of the resin.

2. Ion-Exchange Equilibrium Model

Myers and Byington [10] pointed out that for a homogeneous resin the selectivity coefficient was approximately constant at constant ionic strength. Some deviation would be produced by non-idealities of the solution phase or by inhomogeneity in the strength of functional groups of the resin [11, 12]. It has been generally known that crosslinked polymers contain both high and low energy functional groups which may result from the degree of crosslinking and the effect of sulfonation process. In treating this kind of ion-exchange equilibrium, one needs an equilibrium model which takes into account the heterogeneity of the resin. Saunders et al. [8] developed such an equilibrium model based on the findings of Myers and Byington [12]. They assumed a binomial distribution of n+1 type functional groups to characterize the ion-exchange phenomena. The probability of a site of type i is defined as

$$P_i=\binom{n}{i} s^i(1-s)^{n-i},\quad 0<s<1 \tag{7}$$

where s is the skewness of the site distribution function. A characteristic energy level, $E_{i,j}$, for the uptake of an ion j on a site of type i is given by

$$E_{i,j}=\bar{E}_j+\left\{\frac{(i-ns)}{\sqrt{ns(1-s)}}\right\}\sigma_j \tag{8}$$

where $\bar{E}_j$ and σ_j are the average value and the standard deviation of the distribution function of energy.

If the functional groups of the resin are completely dissociated, which is a reasonable assumption for sulfonic acid resins, the following equation may be used to represent the uptake of an ion j on a site i.

$$\frac{Q_{i,j}}{Q_{0i}}=C_{i,j}X_{Aj}/\left(\sum_{k=1}^{N} C_{i,k}X_{Ak}\right) \tag{9}$$

where Q_{0i} is the concentration of site i which is Q_0P_i, and N is the number of exchangeable counterions. The values of $C_{i,j}$ can be expressed in terms of the adsorption energy as

$$C_{i,j}=\bar{C}_j \exp\left\{\frac{(\bar{E}_{i,j}-E_j)}{R_gT}\right\} \tag{10}$$

The total uptake of ion j, therefore, may be obtained by a sum of the products of individual uptake and its probability over all sites

$$Y_{Aj}=\frac{Q_j}{Q_0}=\sum_{i=0}^{n}\left\{\frac{C_{i,j}P_iX_{Aj}}{\sum_{k=1}^{N} C_{i,k}X_{Ak}}\right\} \tag{11}$$

By substituting Eqs. (9) and (11) into Eq. (15), the selectivity of ion j relative to a reference ion r is given by

$$S_{j,r}=\frac{\sum_{i=0}^{n}\left\{\frac{P_i}{\sum_{k=1}^{N} B_{k,j}W_{k,j}^{Ui}X_{Ak}}\right\}}{\sum_{i=0}^{n}\left\{\frac{P_i}{\sum_{k=1}^{N} B_{k,r}W_{k,r}^{Ui}X_{Ak}}\right\}} \tag{12}$$

where

$$B_{k,j}=\frac{\bar{C}_k}{\bar{C}_j} \tag{13}$$

$$W_{k,j}=\exp\left\{\frac{(\sigma_k-\sigma_j)}{RT}\right\} \tag{14}$$

$$U_i=\frac{(i-ns)}{\sqrt{ns(1-s)}} \tag{15}$$

$B_{k,j}$ is the average selectivity of ion k to ion r and $W_{k,j}$ is the heterogeneity. They have the following relationships

$$B_{k,k}=W_{k,k}=1 \tag{16}$$

$$B_{k,j}=\frac{1}{B_{j,k}} \text{ and } W_{k,j}=\frac{1}{W_{j,k}} \tag{17}$$

$$B_{k,j}=B_{k,m}B_{m,j} \text{ and } W_{k,j}=W_{k,m}W_{m,j} \tag{18}$$

Once all the $S_{j,r}$'s are known, the uptake of ion j may be calculated by

$$Y_j=\frac{X_{Aj}S_{j,r}}{\sum_{k=1}^{N} X_{Ak}S_{k,r}} \tag{19}$$

Prior to use Eq. (19) to compute all the amounts taken by the resin, one should determine $B_{k,r}$ and $W_{k,r}$ (after simply denoted by B and W) of all ions to a reference ion. In this study we have used the hyrogen ion as the reference. For a binary system, the selectivity of ion 1 relative to the reference ion r is simply given by

$$S_{1,r}=\frac{\sum_{i=0}^{n}\left\{\frac{BW^{Ui}P_i}{[(BW^{Ui}-1)\ X_{Ai}+1]}\right\}}{\sum_{i=0}^{n}\left\{\frac{P_i}{[(BW^{Ui}-1)\ X_{Ai}+1]}\right\}} \tag{20}$$

With a given set of n and s, B and W can be determined by matching Eq. (20) with experimental equilibrium data by means of a least-square optimization routine.

3. Separation Model

A macroreticular resin particle is schematically shown in Fig. 1 to show mass transfer mechanisms inside the resin particle. Intraparticle mass transport occurs by diffusion through the liquid-filled macropore and into microparticles (or microspheres). A simple kinetic model for the uptake of amino acids would be

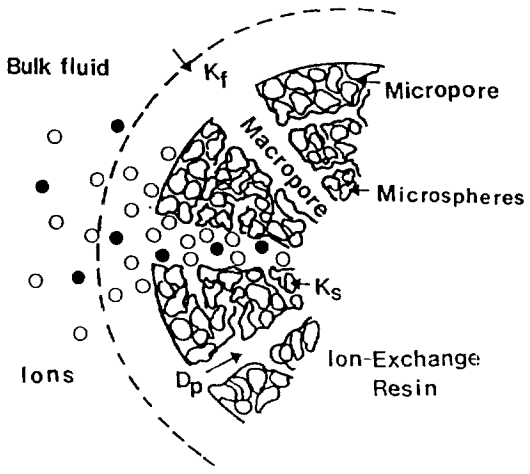

Fig. 1. Schematic diagram of intraparticle mass transfer.

Table 1. Properties of a cation exchanger, Amberlite 200

Property	Amount
Ion-exchange capacity (mol/kg)	4.26(3.35^{+++})
Particle density (kg/m^3)	892(669$^+$)
Packing density (kg/m^3)	580(435$^+$)
Water content (%)	48-50
Degree of crosslinking* (%)	20
Average particle diameter** (10^{-3} m)	0.80
Void fraction of micropore^{++}	0.29
Diameter of microspheres^{++} (μm)	0.0616
Void fraction of bed	0.35
Maximum operating temperature* (℃)	150

*Manufacturer's specification
**16/50 mesh, mixed particles
$^+$After swelling
$^{++}$Yoshida et al. [9]
$^{+++}$After regeneration

developed based on the following assumptions.

(1) The ion-exchange resin particle is composed of porous microspheres [9, 10].

(2) Coions can freely move through macropores, but they are excluded from the microspheres by the Donnan potential effect [8].

(3) While all types of amino acids can diffuse through macropores, only their cations can move into microparticles [8-10].

(4) Local equilibrium exists between the macropore fluid and microspheres [3, 13].

(5) A linear driving force approximation (LDFA) is possible for transport through microspheres since they are quite small [13]. According to the assumptions above, the mass balance equation around a resin particle is given by

$$\frac{\partial C_{pi}}{\partial t}=\frac{D_{pi}}{R^2}\frac{\partial}{\partial R}\left(R^2\frac{\partial C_{pi}}{\partial R}\right)-\frac{\rho_p}{\varepsilon}\frac{\partial \bar{Q}_i}{\partial t} \tag{21}$$

where C_{pi} is the fluid phase concentration in macropores and $\bar{Q}_i$ is the volume-averaged solid phase concentration in microspheres which is a function of time and R. D_{pi} is the macropore diffusion coefficient. It has been generally accepted that the positively charged amino acid has the same diffusion coefficient as the neutral one has. Initial and boundary conditions for Eq. (21) are as follows

$$C_{pi}(R,\ 0)=C_{pi}^0 \tag{22}$$

$$\frac{\partial C_{pi}}{\partial R}=0 \qquad \text{at } R=0 \tag{23}$$

$$\varepsilon D_{pi}\frac{\partial C_{pi}}{\partial R}=k_{fi}(C_{bi}-\bar{C}_{pi}) \qquad \text{at } R=R_0 \tag{24}$$

where $\bar{C}_{pi}$ is the fluid phase concentration at the outer surface of microspheres which is in equilibrium with $\bar{Q}_i$; k_{fi} is the external film mass transfer coefficient; and R_0 is the radius of the spherical resin particle. The average concentration in the microspheres is simply given by the LDFA [13]

$$\frac{\partial \bar{Q}_i}{\partial t}=k_{si}(Q_{si}-\bar{Q}_i) \tag{25}$$

$$\bar{Q}_i(R,\ 0)=Q_i^0 \tag{26}$$

where k_{si} is the solid phase mass transfer coefficient for the transport through microspheres.

When one uses a finite batch adsorber, a mass balance equation in the batch is required as follows

$$V\frac{dC_{bi}}{dt}=-k_{fi}a[C_{bi}-C_{pi}(R_0)] \tag{27}$$

$$C_{bi}(0)=C_{bi}^0 \tag{28}$$

where a is the external surface area of the resin particle which can be calculated from

$$a=\frac{3w}{\rho_p R_0} \tag{29}$$

where w is the weight of the resin particles charged in the batch adsorber and ρ_p is the particle density.

In general, the determination of parameters in the model equation can be done by matching the experimental concentration curve with the predicted curve from the model. Eqs. (21)-(29), coupled with the ion-exchange equilibrium model, should be solved to predict the concentration curve. In this work, the set of equations was solved numerically by an orthogonal collocation technique [14]. The detailed procedures are given elsewhere, in a thesis by Kim [15].

EXPERIMENTAL

1. Materials

A macroreticular sulfonated polystyrene-DVB resin, Amberlite 200, manufactured by Rohm & Haas (U. S. A) was used as a cation exchanger. The supplied resin was a sodium form. It was converted to hydrogen form by repeated washing with NaOH and HCl solutions, treating it with a 1.0 N HCl solution, and throughly rinsing with distilled and deionized water. The total ion-exchange capacity was determined by letting a given amount of the hyrogen form resin be in equilibrium with an excess volume of a 0.1 N NaOH solution containing 50 g/L NaCl. After equilibrium was reached, the amount of excess NaOH left in the solution was determined by titration with a 0.1 N HCl solution. The water content of swollen resin particles was measured by the weight loss of preweighted samples that occured by drying in a vaccum oven at 110℃. The average particle radius was measured by an optical microscope with scale. Particle and packing densities and

Table 2. Properties of amino acids used at 25°C

Properties	Phe	Tyr
Solubility in water (kg/m^3)	29.6	0.453
Molecular weight	165.2	181.2
pK1	1.83	2.20
pK2	9.13	9.11
pK3	-	10.07
pI	5.48	5.65
Decompositon temp. (℃)	283	342

particle porosity were determined by conventional methods. Other properties, which could not be measured, were collected from the manufacturer's specifications and the literature [9]. The typical properties of Amberlite 200 are listed in Table 1.

Amino acids studied here are L-phenylalanine (Phe) and L-tyrosine (Tyr), which have quite similar isoelectric points, 5.48 and 5.65, respectively. Both amino acids were purchased from Sigma and used without further purification. The properties of Phe and Tyr are listed in Table 2.

2. Experimental Methods

Equilibrium amounts of Phe and Tyr taken by the resin were obtained by batch equilibrium experiments. For this purpose, 0.1 to 2.0 g of dry resin was put into flasks and allowed to reach equilibrium with a known concentration. The flasks were placed in a constant temperature shaking bath at 25℃. Three days were enough for the system to reach equilibrium. The concentrations of amino acids were measured by means of UV spectrometry. Wavelengths used were 255 and 272 nm for Phe and Tyr, respectively. The concentrations of individual species in mixtures were obtained by solving the corresponding Beer-Lambert equation with calibration constants in the concentration range in which calibration curves are represented by straight lines [15]. Ion-exchange experiments were carried out in a finite batch adsorber of 2 L and about 2 g of the resin was loaded into four cages made of 80 mesh stainless-steel acreen and the cages were affixed to the rotating shaft to permit good contact with the solution. All the experiments were carried out at approximately 500 rpm so that the external film mass transfer coefficient, k_f, would be nearly constant. The solution pH was also adjusted to elucidate the effect of pH on the uptake of amino acids. The batch adsorber was placed in a constant temperature water bath to maintain at 25℃.

RESULTS AND DISCUSSION

1. Ion-exchange Equilibria

According to the solution equilibria shown in the previous section, the concentration of amino acid cations decreases with the value of pH, but the relative ionic fraction of amino acid cations increases because the concentration of the hydrogen ion decreases. In general, it has been known that the ionic fraction of amino acid cations gradually increases with pH, reaches a maximum at their isoelectric pH, and abruptly decreases to zero in basic solutions as shown in Fig. 2. The uptake of an amino acid has the same tendency as the ionic fraction has. This fact implies that ion-exchange phenomena come from the competition between two counter ions in the solution, so that the uptake of an ion depends on its relative fraction and ionic strength. When a cation exchanger is used as a separating medium, it can not take up amino acids

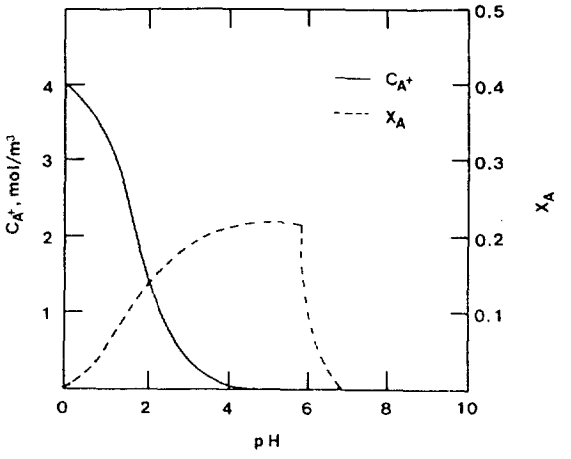

Fig. 2. Ionic fraction and concentration of positive Phe in terms of solution pH.

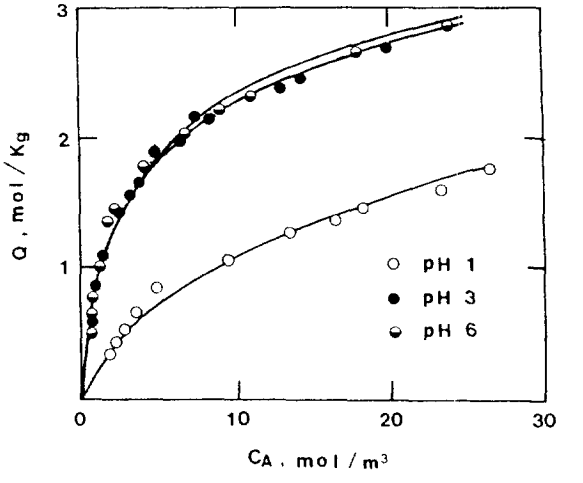

Fig. 3. Uptake of Phe as a function of total equilibrium concentration and solution pH.

in the basic solution. This can be explained by the Donnan potential effect, where all negatively charged ions are excluded from the resin.

In ion-exchange processes, there is at least one counter ion, namely the hydrogen ion in aqueous solutions. Therefore the system becomes binary from the point of physics when amino acids are concerned. Figs. 3 and 4 show the ion-exchange isotherms of Phe and Tyr obtained by varying the solution pH. As mentioned already, the uptake of amino acids reaches maximum around their isoelectric pH and is quite low at pH=1 because of strong competition with hydrogen ions. Fig. 5 shows a theoretically calculated uptake curve of Phe in terms of pH when the liquid phase equilibrium concentration is fixed as 3 mol/m^3. This curve is similar to the curve for the ionic fraction shown in Fig. 2. In the range of pH from 1 to 3, the uptake increases but it remains nearly constant after pH=3. In basic solutions, the uptake should be zero since all amino acids are negatively charged. This characteristic makes a cyclic separation process for amphoteric substances such as amino acids possible. According to the above results, it may be concluded that ion-exchange is the predominant uptake mechanism and nonionic adsorption does not occur to a significant

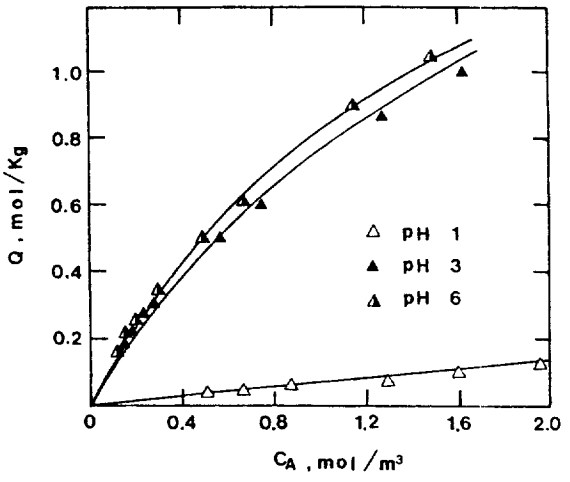

Fig. 4. Uptake of Tyr as a function of total equilibrium concentration and solution pH.

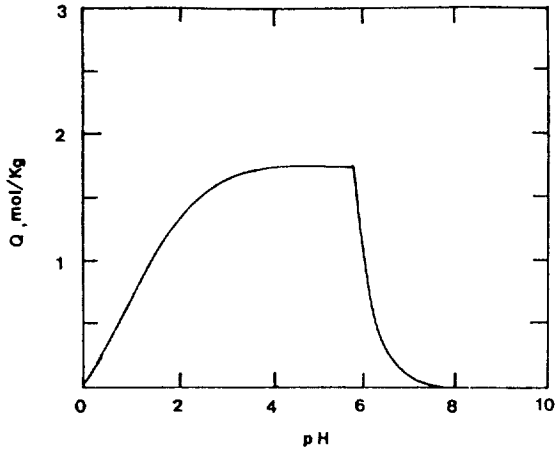

Fig. 5. Effect of pH on equilibrium uptake of Phe in batch separator.

extent under the conditions used in this work.

The best fit values of B and W for each amino acid were determined from experimental isotherms by using a least-square optimization routine, minimizing the object function which sums up the squared deviation between the experimental uptake and its corresponding value predicted by Eq. (20) at all experimental points. Here the hydrogen ion, the least preferred ion, was used as the reference ion. In determining B and W, the skewness of the site distribution function, s, was assumed to be 0.5 which means a symmetrical site distribution. The number, n, was assumed to be from 2 to 4. This assumption is chosen as a matter of convenience since we do not have sufficient information on the site distribution of the resin. The best fit values of B and W determined with varying values of n are given in Table 3. The solid lines in Figs. 3 and 4 are calculated from the ion-exchange equilibrium model with the best fit parameters when n=2 as listed in the table.

2. Estimation of Mass Transfer Coefficients

In the mass balance equations, there are two mass transfer coefficients besides the macropore diffusion coefficient. The first is the external film mass transfer coefficient, k_f, and the second is the solid phase mass transfer coefficient, k_s, for microspheres.

Table 3. Ion-exchange equilibrium parameters of Phe and Tyr at 25°C with s=0.5

		n=1	n=2	n=4
Phe	B	1.880	2.108	2.219
	W	5.984	5.401	5.561
Tyr	B	1.050	1.176	1.254
	W	3.094	2.712	2.467

Table 4. Diffusion and mass transfer coefficients obtained

Species	C_0 (mol/m³)	w/V (kg/m³)	$D_p \times 10^9$ (m²/s)	$k_f \times 10^5$ (m/s)	k_s (s^{-1})
Phe	4.011	1.100	4.200	4.86	0.98
	4.144	0.950	3.400	3.82	
Tyr	0.987	0.950	6.500	6.56	1.12
	0.998	0.950	4.500	3.75	

There are a few correlations for estimating the external film mass transfer coefficient in batch systems [16, 17]. In most of the adsorption processes where highly porous sorbents are used, the solution-particle mass transfer resistance may be neglected when comparing it with that of intraparticle diffusion. However, it is important to estimate the order of magnitude. In this work, we estimated k_f from the initial concentration history in which the diffusional resistance does not significantly prevail. The initial concentration history may be approximated by Eq. (30) when the adsorption time is less than 300 seconds [3].

$$\ln(C/C_0) = -3k_f wt/\rho_p R_0 V \quad (30)$$

where V is the volume of solution, w is the weight of sorbent particles loaded and ρ_p is the particle density in the swelling state. The values of k_f obtained are $3.75-6.56\times10^{-5}$ m/s as shown in Table 4.

The mass transport through microspheres may be simplified by introducing the LDFA [13, 19]. In this case, the solid phase mass transfer coefficient can be estimated from the well known equation

$$k_{si} = 15\ D_{si}/r_0^2$$

where D_{si} is the solid diffusion coefficient and r_0 is the radius of the microspheres.

In this study, D_{si} and r_0 were collected from the literature and used to estimate the value of k_{si}. Saunders et al. [8] used a kinetic model based on parallel diffusion through liquid-filled macropores of resin and through microspheres and reported the diffusion coefficients of Phe and Tyr through micropores of Amberlite 252. The diameter of microspheres of Amberlite 200 was reported to be 0.0616 μm [9]. According to approximate values of D_{si} and r_0, the solid phase mass transfer coefficients of Phe and Tyr were estimated to be about 1.0 s^{-1} as shown in Table 4.

3. Macropore Diffusion Coefficients

Since macropore diffusion is usually the rate-controlling step in most ion-exchange processes, the determination of macropore diffusion coefficients is an important task. There are various methods for determining the diffusion coefficient in the literature [3, 18]. The most general method is to compare the experimental concentration curve and the predicted one by using the specified diffusion model. Since the diffusion coefficient, which is obtained

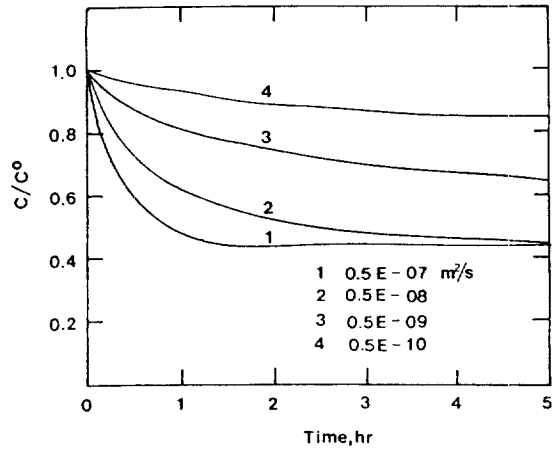

Fig. 6. Sensitivity of D_p on concentration history of Phe.
$C^0=1.000$ mol/m^3 and w/V=1.000 kg/m^3 with $k_f=5.0\times10^{-5}$ m/s and $k_s=1.0$ s^{-1}

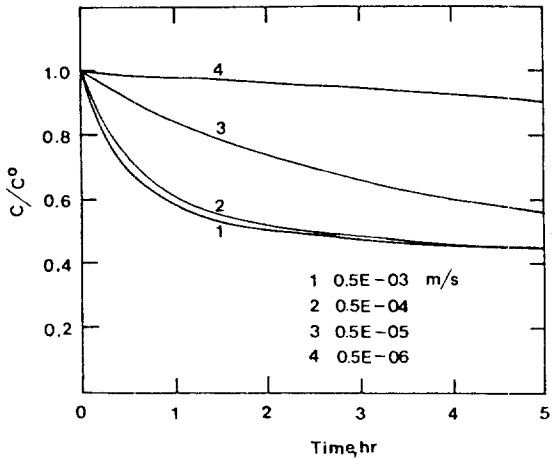

Fig. 7. Sensitivity of k_f on concentration history of Phe.
$C^0=1.000$ mol/m^3 and w/V=1.000 kg/m^3 with $D_p=5.0\times10^{-9}$ m^2/s and $k_s=1.0$ s^{-1}

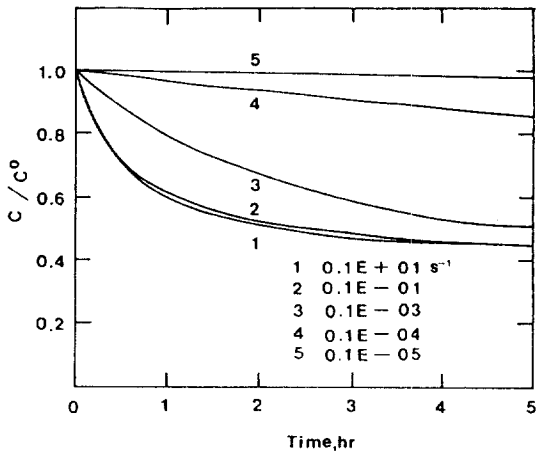

Fig. 8. Sensitivity of k_s on concentration history of Phe.
$C^0=1.000$ mol/m^3 and w/V=1.000 kg/m^3 with $D_p=5.0\times10^{-9}$ m^2/s and $k_f=5.0\times10^{-5}$ m/s

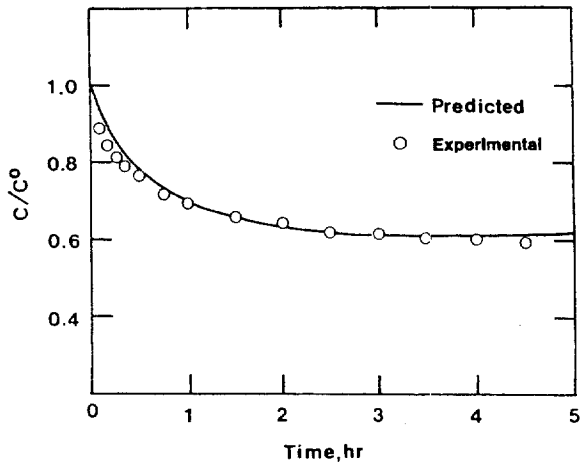

Fig. 9. Concentration history of Phe at pH=6.0.

by this method, reflects all kinds of mass transfer resistances inside a particle, it has been called the effective diffusion coefficient.

The determined macropore diffusion coefficients of Phe and Tyr are in the range of $3.4-6.5\times10^{-9}$ m^2/s. There are 2 or 3 times of free molecular diffusion coefficients in dilute aqueous solutions, 1.95 and 2.0×10^{-9} m^2/s, respectively. This implies that other transfer mechanisms also occur along with macropore diffusion.

4. Sensitivity Test of Model Parameters

Sensitivities of model parameters on the concentration curve have been checked to show how a mass transfer mechanism affects the overall uptake rate. For this purpose, we chose typical values of k_f, D_p, and k_s as 5.0×10^{-5} m/s, 5.0×10^{-9} m^2/s, and 1.0 s^{-1}, respectively. Figs. 6-8 show the sensitivities of each rate parameter by adjusting the order of magnitude when other parameters are fixed with their typical values. If concentration curves around the typical value of a parameter are significantly changed, it may be qualitatively concluded that the parameter affects greatly the overall uptake rate. According to the results shown in the Figs. 6-8, k_f and D_p have considerable effect on the concentration curve, but k_s gives little change to the concentration curve when it is greater than 0.1 s^{-1}. This result implies that external mass transfer and macropore diffusion are major transport mechanisms for the uptake of amino acids by Amberlite 200 and the assumption which we made for the diffusion through micopores is quite reasonable. In a sense, the mass transfer resistance through micropores can be neglected since it has only a maginal effect on the concentration curve. In this case, one can simulate or predict the dynamic behavior of amino acids in a finite batch or a fixed-bed adsorber simply by means of a simple kinetic model, considering only the film-macropore diffusion.

5. Concentration Curves

As mentioned already, a separation model was formulated by combining the ion-exchange equilibrium model into a set of mass balance equations. In order to verify the applicability of the model, concentration curves of Phe and Tyr were predicted by the proposed separation model above. Figs. 9 and 10 show experimental concentration curves of Phe at a given condition. The solid lines represent the prediction by the separation model. The last part of the calculated concentration curve depends on the ion-exchange equilibrium. Deviations between experimental and calcu-

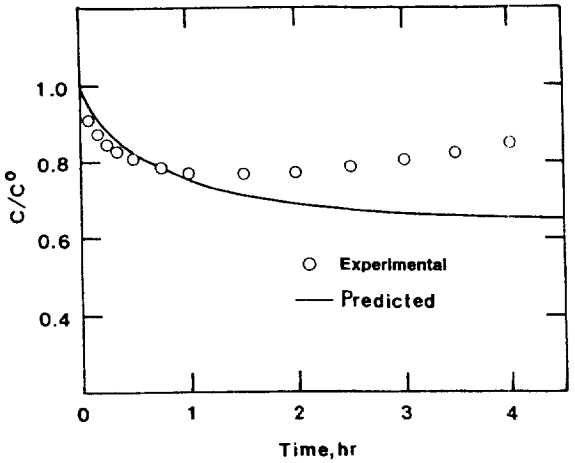

Fig. 10. Concentration history of Phe at pH=2.0.

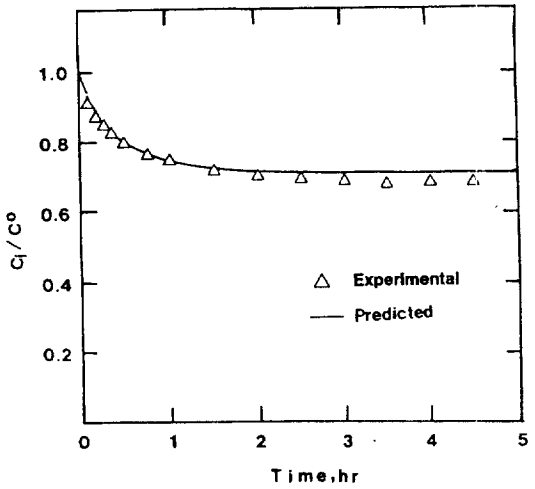

Fig. 11. Concentration history of Tyr at pH=2.0.

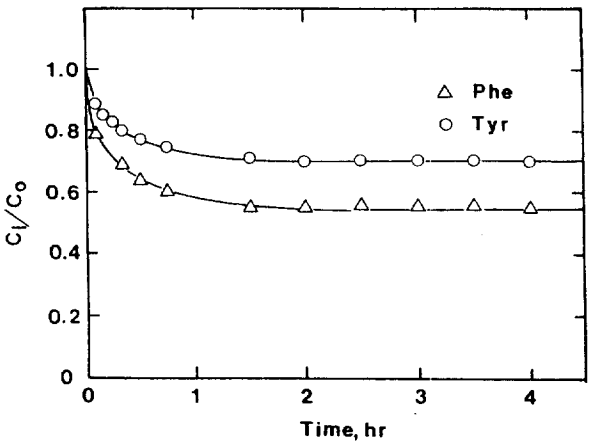

Fig. 12. Binary concentration history for Phe/Tyr system at pH=6.0.

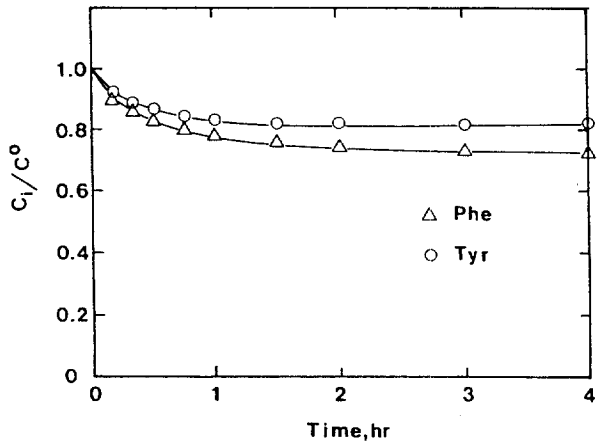

Fig. 13. Binary concentration history for Phe/Tyr system at pH=2.0.

lated results in this part come from the error in the equilibrium model. Fig. 11 shows the result for Tyr at pH=2.

For single amino acids, the separation model predicts quite satisfactorily the concentration curves. However, we found a peculiar phenomenon in the experimental concentration curves of Phe at low pH values. At pH less than 2, the uptake of Phe occurs smoothly for 1-2 hours and then the resin desorbs a certain amount of Phe later on. This kind of phenomenon was found in other experiments under similar conditions mentioned above. Due to insufficient data we could not go deeply into this matter. However, we may think that the change in pH during the ion-exchange process will make a significant effect on the ion-exchange equilibrium. We found that there was a considerable change in pH during the uptake experiments for Phe when the initial pH value is low. This phenomenon can be controlled by adjusted the pH value during experiments or by adding a buffer solution. We did not use a buffer solution to get rid of any side effects from other counter ions. According to the results, it became evident that the isolation of an amino acid from mixtures should be done at a pH value near its isoelectric pH.

We also conducted some experiments for mixed amino acids or ternary ionic systems shown in Figs. 12 and 13. However, we failed to predict the mixed concentration curves because of the limitation of the ion-exchange equilibrium model extended in this study. In principle, the extended equilibrium model can be applied to all systems regardless of the number of amio acids in the mixture but it does not give good predictions for mixed amino acids. To solve this problem, one needs to try a new approach considering ionic activities in the solution and ionic interactions in the resin as well as the effect of structural heterogeneity.

CONCLUSIONS

As a separation and recovery method for amino acids, the ion-exchange of L-phenylalanine and L-tyrosine was carried out in a finite batch adsorber loaded with a cation exchange resin, Amberlite 200. The uptake of an amino acid depends on its ionic fraction and becomes maximum at its isoelectric pH. This can be explained by the competition between counter ions, amino acid cations and hydrogen ions, in the solution. An ion-exchange equilibrium model which took into account the structural heterogeneity of resins was extended for mixed amino acids. A kinetic model was formulated based on a consecutive transport mechanism, the external film mass transfer, the diffusion through the liquid-filled macropores, and the transport through microparticles. Since microparticles are quite small, the last step occurs very fast. The overall uptake rate depends on external film mass transfer and macropore diffusion. Such a fact makes it possible to use

a simple separation model to predict and simulate the ion-exchange behavior. The separation model, which was made by combining the ion-exchange equilibrium model and the kinetic model, can be used satisfactorily for binary ionic systems but it does not give good predictions for ternary ionic systems or mixed amino acids because of the limitation of the extended ion-exchange equilibrium model.

ACKNOWLEDGEMENT

This research was supported by the Korea Science and Engineering Foundation under grant No. 921-1000-014-1.

NOMENCLATURE

- a : interfacial area between fluid and resin particles [m^2]
- $B_{i,j}$: average binary separation factor for ion i relative to ion j
- C : liquid-phase solute concentration [mol/L or mol/m^3]
- C_0 : unit or initial liquid-phase concentration [mol/m^3]
- $C_{i,j}$: equilibrium constant for ion j on site i
- D_p : macropore effective diffusion coefficient [m^2/s]
- D_s : microparticle effective solid diffusion coefficient [m^2/s]
- $E_{i,j}$: adsorption energy for ion j on site i [J/mol]
- $\bar{E}_j$: average adsorption energy of ion j [J/mol]
- K_1 : first dissociation equilibrium constant [mol/m^3]
- K_2 : second dissociation equilibrium constant [mol/m^3]
- k_f : film mass transfer coefficient [m/s]
- k_s : solid-phase mass transfer coefficient [s^{-1}]
- n : number of sites-1
- P_i : probability distribution of site type i
- Q : resin equilibrium uptake, mol/kg dry resin
- Q_0 : resin ion-exchange capacity, mol/kg dry resin
- R : particle radial coordinate [m]
- R_0 : particle radius [m]
- r_0 : radius of microspheres [m]
- $S_{i,j}$: separation factor for ion i relative to ion j
- s : skewness parameter of site distribution
- t : time [s or hr]
- U_i : parameter defined in Eq. (15)
- V : solution volume [m^3]
- w : weight of resin charged [kg]
- $W_{i,j}$: heterogeneity parameter defined in Eq. (14)
- X_A : liquid-phase ionic fraction
- Y_A : resin-phase ionic fraction

Greek Letters

- ε : bed porosity
- ρ_p : apparent particle density [kg/m^3]

REFERENCES

1. Blackburn, S.: "Amino Acids and Amines", Handbook of Chromatography, Zweig, G., Sherma, J. Ed., CRC Press, Boca Raton, 1983.
2. Costa, C. and Rodrigues, A. E.: *AIChE J.*, **31**, 1645 (1985).
3. Moon, H., Kook, S. K. and Park, H. C.: *Korean J. Chem. Eng.*, **8**, 168 (1991).
4. Seno, M. and Yamabe, T.: *Bull. Chem. Soc. Japan*, **34**, 102 (1961).
5. Fieitelson, J.: *J. Phys. Chem.*, **67**, 2544 (1963).
6. Yu, Q. and Wang, N. H. L.: *Sep. Purif. Meth.*, **15**, 127 (1986).
7. Yu, Q., Yang, J. and Wang, N. H. L.: *React. Polym.*, **6**, 33 (1987).
8. Saunders, M. S., Vierow, J. B. and Carta, G.: *AIChE J.*, **35**, 53 (1989).
9. Yoshida, H., Kataoka, T. and Ikeda, S.: *Can. J. Chem. Eng.*, **63**, 430 (1985).
10. Myers, A. and Byington, S.: "Ion Exchange Science and Technology", Rodrigues, A. E., Ed., NATO ASI, Series E., No. 107, Nijhoff, Dordrecht (1986).
11. Patell, S. and Turner, J. C. R.: *J. Sep. Proc. Technol.*, **1**, 42 (1979).
12. Patell, S. and Turner, J. C. R.: *J. Sep. Proc. Technol.*, **1**, 31 (1980).
13. Moon, H. and Lee, W. K.: *Chem. Eng. Sci.*, **41**, 1995 (1986).
14. Villadsen, J. and Michelsen, M. L.: "Solution of Partial Differential Equation Models by Polynomial Approximation", Prentice-Hall, Englewood Cliffs (1978).
15. Kim, C. M.: "Transport of Amino Acids in a Cation Exchanger", M. S. Thesis, Chonnam National Univ., Kwangju (1994).
16. Teshima, H. and Ohashi, Y.: *J. Chem. Eng. Japan*, **10**, 70 (1977).
17. Misic, D. M., Sudo, Y., Suzuki, M. and Kawazoe, K.: *J. Chem. Eng. Japan*, **15**, 67 (1982).
18. Moon, H. and Lee, W. K.: *J. Colloid Interface Sci.*, **96**, 162 (1983).
19. Huang, T. and Cho, L.: *J. Chem. Eng. Japan*, **21**, 498 (1988).